Analysing the atolls

Gladstone, Jeanette; Done, Chris; Gierliński, Marek

Published in:
Monthly Notices of the Royal Astronomical Society

DOI:
10.1111/j.1365-2966.2007.11675.x

Publication date:
2007

Licence:
Unspecified

Document Version
Publisher's PDF, also known as Version of record

Mon. Not. R. Astron. Soc. **378,** 13–22 (2007) doi:10.1111/j.1365-2966.2007.11675.x

Analysing the atolls: X-ray spectral transitions of accreting neutron stars

Jeanette Gladstone,[1⋆] Chris Done[1] and Marek Gierliński[1,2]
[1]*Department of Physics, University of Durham, South Road Durham DH1 3LE*
[2]*Obserwatorium Astronomiczne Uniwersytetu Jagiellońskiego, 30-244 Kraków, Orla 171, Poland*

Accepted 2007 February 27. Received 2007 February 21; in original form 2006 February 27

ABSTRACT

We systematically analyse all the available X-ray spectra of disc accreting neutron stars (atolls and millisecond pulsars) from the *RXTE* data base. We show that while all these have similar spectral evolution as a function of mass accretion rate, there are also subtle differences. There are two different types of hard/soft transition, those where the spectrum softens at all energies, leading to a diagonal track on a colour–colour diagram, and those where only the higher energy spectrum softens, giving a vertical track. The luminosity at which the transition occurs is *correlated* with this spectral behaviour, with the vertical transition at $L/L_{\rm Edd} \sim 0.02$ while the diagonal one is at $\sim$0.1. Superimposed on this is the well-known hysteresis effect, but we show that classic, large-scale hysteresis occurs only in the outbursting sources, indicating that its origin is in the dramatic rate of change of mass accretion rate during the disc instability. We show that the long-term mass accretion rate correlates with the transition behaviour, and speculate that this is due to the magnetic field being able to emerge from the neutron star surface for low average mass accretion rates. While this is not strong enough to collimate the flow except in the millisecond pulsars, its presence may affect the inner accretion flow by changing the properties of the jet.

Key words: accretion, accretion discs – X-rays: binaries.

1 INTRODUCTION

Neutron stars represent the most dense form of matter known before black hole formation. The equation of state of such material is not well understood but typical expected size scales of $R \sim 10$ km for a $1.4\,{\rm M}_{\odot}$ object give M/R similar to that of the last stable orbit around a Schwarzschild black hole. The gravitational potential seen by the accreting material is then very similar in neutron stars and black holes, but with the obvious difference that the material may then fall seamlessly and invisibly from the edge of the disc through the event horizon in the black holes (but see e.g. Krolik, Hawley & Hirose 2005 for an alternative view), but must impact on to the solid surface for the neutron stars. This boundary layer emission should give a clear distinction between the two types of systems, yet in practice it can be quite hard to discriminate between the disc accreting, low magnetic field neutron stars and Galactic black holes (GBH). Both show hard spectra at low mass accretion rates (e.g. Barret & Vedrenne 1994; Barret et al. 2000) while at higher mass accretion rates the black holes can show low temperature, optically thick Comptonized emission from a corona which can look similar to an optically thick boundary layer in the neutron stars systems (the black hole 'very high state'; Done & Gierliński 2003, hereafter DG03).

⋆E-mail: j.c.gladstone@durham.ac.uk

None the less, DG03 showed that there are clear differences between the black hole and neutron star systems. They used the huge data base now available on these objects from the *Rossi X-ray Timing Explorer* (*RXTE*) to build a picture of the X-ray spectral evolution as a function of overall mass accretion rate (as measured by luminosity, parametrized in units of the Eddington rate, $L/L_{\rm Edd}$). They used data from GBH and both subclasses of disc accreting, low magnetic field neutron stars namely atolls and *Z* sources (see e.g. Hasinger & van der Klis 1989). The atolls and GBH cover the same luminosity range in $L/L_{\rm Edd}$, from $\sim 10^{-3}$ to $\sim$0.5–1, so their accretion flows should be directly comparable (*Z* sources are typically more luminous, and may have residual magnetic fields: Hasinger & van der Klis 1989). DG03 showed that the GBH as a class were all consistent with the same spectral evolution as a function of mass accretion rate, as were the atolls, but that this behaviour *differed substantially* between the two types of system even though they covered the same range in $L/L_{\rm Edd}$.

DG03 interpreted this in the light of the recent advances in accretion flow models, which suggest that at low mass accretion rates the optically thick, cool, inner disc can evaporate into an optically thin, hot flow (e.g. an advection-dominated accretion flow: Narayan & Yi 1996 or a jet-dominated accretion flow: Falcke, Körding & Markoff 2004). These models are currently controversial as they conflict with the occasional detection of extremely broad iron lines in GBH spectra in this state (Miller et al. 2002, 2006; Miniutti, Fabian & Miller 2004), though these extreme widths could also be

an artefact of complex absorption (Done & Gierliński 2006). None the less, the truncated disc/hot inner flow models are very attractive as they can qualitatively explain a wide range of observed properties in X-ray binaries. This includes the spectral evolution of the GBH, which can be broadly explained by the transition radius between the disc and hot flow progressively decreasing as the mass accretion rate increases, while the atolls are consistent with an identical accretion flow behaviour but with the addition of the expected boundary layer/surface emission (DG03).

These observational differences between GBH and atolls are consistent with the existence of the event horizon, the most fundamental predicted property of a black hole (see also Sunyaev & Revnivtsev 2000; Garcia et al. 2001; Narayan & Heyl 2002; McClintock, Narayan & Rybicki 2004). However, the sample of atolls used by DG03 was fairly small, with only four objects (one of which was an accreting millisecond pulsar). This contrasts with their GBH selection, which included all available objects which were not heavily absorbed. Here, we present a much wider study using all the available atolls in the *RXTE* data base which are not heavily absorbed to investigate their behaviour in more detail. We find that while all the atolls (and millisecond pulsars) broadly show the same spectral evolution, there are some subtle differences. Some of these can be connected to spin/inclination effects, but there are also some differences in transition behaviour which correlate with long-term mass accretion rate. We speculate that these may be linked through the jet being affected by any remnant polar magnetic field, which in turn depends on the accretion rate.

2 SAMPLE SELECTION AND DATA ANALYSIS

We searched the *RXTE* data base for low magnetic field, disc accreting neutron star systems. We do not include *Z* sources (Sco X−1, GX349+2, GX17+2, Cyg X−2, GX5−1, GX340+0, e.g. Kuulkers et al. 1996, Cir X−1, LMC X-2, Hasinger & van der Klis 1989) as we were interested in the range $10^{-3} < L/L_{\rm Edd} < 1$ to compare with the GBH from DG03. We also exclude all objects with heavy absorption, defined as $N_{\rm H} > 3 \times 10^{22}\,{\rm cm}^{-2}$, as above this the spectral decomposition becomes more uncertain. Given that most systems are in the Galactic plane, this removes many objects (4U 1624−49, GRO J1744−28, GRS 1747−312, SAX J1747.0−2853). The absorption criteria also exclude objects where there is substantial intrinsic absorption. This can be continuous, completely blocking our view of the continuum source so that only the scattered flux is seen (the accretion disc corona sources), or the absorption can be episodic, giving discrete dips in the light curve (the dippers). We exclude all accretion disc corona sources (2S 0921−630, 4U 1624−49, 4U 1822−371, MS 1603+206) and dippers where the absorption events are so frequent that most observations are affected by them (EXO 0748−676), but we do include dippers where the absorption is limited to contaminating only a few observations (which we remove, see next section). Details of all included sources are shown in Table 1.

3 SPECTRAL EVOLUTION OF ATOLLS AND MILLISECOND PULSARS

The standard products spectra (and associated background and response files) from the Proportional Counter Array (PCA), available from the High Energy Astrophysics Science Archive Research Centre (HEASARC) data base, were gathered for each source, giving a total of over 3000 spectra. Following DG03, we fit these with a model of the disc emission and a Comptonized continuum, described by DISKBB (Mitsuda et al. 1984) and THCOMP (Zdziarski, Johnson & Magdziarz 1996) in XSPEC, together with a smeared edge and Gaussian line to approximately mimic the reflected spectrum. The absorption was fixed at the Galactic value for each object (see Table 1). This model gave a good fit to all the spectra ($\chi^2_\nu < 1.5$).

Following DG03, the best-fitting model to each spectrum was integrated to form intrinsic soft and hard colours (i.e. absorption corrected and independent of the instrument response), defined as flux ratios in the bandpasses 4–6.4/3–4 and 9.7–16/6.4–9.7 keV, respectively. The unabsorbed model was also used to estimate the bolometric flux in the 0.01–1000 keV bandpass, and this converted into a luminosity using the distance estimate given in Table 1. As discussed by DG03, the colours are fairly robust to changes in the model spectra as long as the source is not heavily absorbed and the advantage of using intrinsic colours (as opposed to the more widely used instrument colours) is that many objects can be directly compared on the same plot. The bolometric fluxes are more uncertain, as the model is extrapolated outside of the observed energy bandpass. None the less, this model corresponds to expected physical components, and we fix a lower limit to the disc temperature of $\geqslant$0.4 keV and an upper limit to the Comptonizing temperature of $\leqslant$100 keV so the continuum components cannot produce arbitrarily large luminosities in the unobserved energy ranges (DG03).

We identify and exclude data contaminated by dips and X-ray bursts by using the Standard 1 light curves (0.125 s time resolution) corresponding to each Standard 2 spectra. We used the intrinsic rms variability as a tracer of these. All light curves with rms above 50 per cent were inspected for bursts, while the 16-s rebinned light curves were checked for dips if their rms was above 20 per cent. Observations were also excluded if they were contaminated by Galactic ridge emission, seen as a softening of the spectra and large iron line contribution at the lowest luminosities in objects with low Galactic latitude (see e.g. Wardziński et al. (2002) for an example of this in the black hole GX339−4). Fig. 1 shows the resulting colour–colour and colour–luminosity diagram for all 34 atolls and 6 millisecond pulsars combined together. One interesting thing to note is that several atoll sources approach or even exceed Eddington luminosities [4U 1735−44; 4U 1744−26 (GX 3+1); 4U 1758−20 (GX 9+1); XTE J1806−246: Gladstone 2006], showing that the high-luminosity sources are not necessarily *Z* sources (Hasinger & van der Klis 1989).

Fig. 1(a) shows that while the atolls show the same overall behaviour as claimed by DG03, they also show subtle but significant differences. This is most evident in terms of the spectral evolution during the transition between the hard (island) and soft (banana) spectral states, which forms the middle branch of the total *Z*-shaped track on the colour–colour diagram (even though these are atolls, not *Z* sources; see Gierliński & Done 2002; Muno, Remillard & Chakrabarty 2002). We have highlighted this by picking out in red those objects where the transition makes an almost vertical track on the colour–colour diagram (hereafter called verticals), while the blue symbols show those where the transition from island to banana starts much further to the right on the colour–colour diagram, but ends at approximately the same place, making a much more diagonal middle branch (hereafter called diagonals). This difference in spectral evolution is also picked out in the colour–luminosity diagram as a different luminosity for the hard–soft transition. While the distances are generally rather uncertain, this correlation between the behaviour on the colour–colour and colour–luminosity diagrams gives some confidence in the reality of the luminosity difference. We stress that this is not primarily due to hysteresis, the well-known effect in both black holes and neutron stars where the luminosity

Table 1. A list of atoll (above the dividing line) and millisecond pulsar (below the line) sources with observations available from the *RXTE* data base. Letters in Column 4 refer to: P – persistent, ST – transient (can be recurrent), LT – long-term transients (outburst >3 month), found using the RXTE Galactic Centre Observations (http://lheawww.gsfc.nasa.gov/users/craigm/galscan/main.html) and the RXTE ASM Weather Map definitive light curves (http://heasarc.gsfc.nasa.gov/xte_weather). Classifications marked asterisk (*) denote sources for which long-term light curves were not available. In this case, classifications were obtained via refereed articles. Letters in Column 5 refer to B – banana (soft) state only, I – island (hard) state only, T – transitions between both states.

Source name	Alternate name	$N_{\rm H}$ (10^{22} cm^{-2})	Distance (kpc)	Persistent or transient	PCA state or transition	Dips	Period (hr)	Spin (Hz)	References
4U 0614+091		0.28	3	P	T		0.25		1,2,4
4U 0919−54	2S 0918−549	0.32	4.9	P	T		0.42		4,6,7
4U 1254−690	GR Mus	0.291	13	P	B	Y	3.9		1,3,8,9,10,11
4U 1543−624		0.27	7	P	B		0.3		3,4,7,12,13,14
4U 1556−605		0.296	4	P	B		9.1		1,3
4U 1608−52	GX 331−01	1.5	3.6	ST	T		288	619	1,3,15,16,17
4U 1626−67		0.069	8	P	I		0.68		18,19,20
4U 1636−53		0.37	5.9	P	T		3.9	582	1,15,21
4U 1702−43	Ara X-1	1.2	7.3	P	T			330	1,3,5,8
4U 1704−30	MXB 1659−298	0.35	12	LT	T	Y	4.2	567	22,23,24
4U 1705−44		1.47	7.4	P	T				1,3,25
4U 1708−40		2.9	8	P	B				26
4U 1711−35	2S 1711−339	1.5	8	ST	T				1,27
4U 1724−307		1	6.6	P	T				1,28,29
4U 1728−16	GX 9+9	0.232	5	P	B				1,2,3,30
4U 1728−34	GX 345−0	2.5	4.75	P	T			363	1,15,31,32,33
4U 1730−33	Rapid burster	1.6	8	ST	B				1,3,34
4U 1735−44		0.46	9.2	P	B		4.65		1,2,3,5,35
4U 1744−26	GX3+1	1.76	8.5	P	B				1,2,3,5
4U 1746−37		0.295	10.7	P	T	Y	5.16		1,3,8,36,37
4U 1758−20	GX 9+1	1.433	8.5	P	B				1,2,3,5
4U 1812−12		1.6	4	P	I				1,38
4U 1820−303		0.24	5.8	P	T		0.19		1,3,39
4U 1837+04	Ser X-1	0.51	8.4	P	B				1,3,5
4U 1850−08		0.39	6.8	P	T		0.35		3,40,41
4U 1908+005	Aql X-1	0.96	2.5	ST	T		19	549	1,3,15,17,42
4U 1915−05	2S 1912−05	0.2	9.3	P	T	Y	0.8	272	1,3,8,43,44,45,46
GS 1826−238		2.4	6	P	I		2.1	611	1,47,48,49
KS 1731−26		1	7	LT	T			524	1,15,47,50,51
SLX 1732−304		1.2	15	LT*	B				52,53
SLX 1735−269		1.47	8.5	P	T				1,48,54,55
XTE J1709−267		0.44	8.8	ST	T				56
XTE J1806−246		0.5	8	ST*	T				1,57,58
XTE J2123−058		0.66	8	ST	T				1,59
IGR J00291+5934		2.8	4	ST	I		2.46	599	60,61,62
XTE J0929−314		0.21	10	ST	I		0.73	185	61,63,65
XTE J1751−305		1.01	8	ST	I		0.7	435	61,63,64,65
XTE J1807−294		0.5	8	ST	I		0.67	190	61,63
XTE J1808−369	SAX J1808.4−3658	0.122	3.15	ST	I		2	401	17,61,63,66
XTE J1814−338		0.167	8	ST	I		4.27	314	61,67,68

References are: [1]Liu, van Paradijs & van den Heuvel (2001), [2]Schultz (1999), [3]Christian & Swank (1997), [4]Nelemans et al. (2004), [5]Fender & Hendry (2000), [6]Jonker et al. (2001), [7]Juett & Chakrabarty (2003), [8]Díaz Trigo et al. (2006), [9]Smale, Church & Bałucińska-Church (2002), [10]Courvoisier et al. (1986), [11]in't Zand et al. (2003a), [12]Schultz (2002), [13]Wang & Chakrabarty (2004), [14]Farinelli et al. (2003), [15]Piro & Bildsten (2005), [16]Gierliński & Done (2002), [17]Garcia et al. (2001), [18]Owens, Oosterbroek & Parmar (1997), [19]Chakrabarty (1997), [20]Angelini et al. (1995), [21]Wijnands (2001), [22]Oosterbroek et al. (2001), [23]Wijnands, Strohmayer & Franco (2001), [24]Oosterbroek et al. (2001), [25](Di Salvo et al. 2005), [26]Migliari et al. (2003a), [27]Wilson et al. (2003), [28]Molkov, Grebenev & Lutovinov (2000), [29]Emelyanov et al. (2002), [30]Yao & Wang (2005), [31]Di Salvo et al. (2000), [32]Shaposhnikov, Titarchuk & Haberl (2003), [33]Migliari et al. (2003a), [34]Falanga et al. (2004), [35]Cornelisse et al. (2000), [36]Jonker et al. (2000), [37]Bałucińska-Church et al. (2004), [38]Barret, Olive & Oosterbroek (2003), [39]Shaposhnikov & Titarchuk (2004), [40]Sidoli et al. (2005), [41]Homer et al. (1996), [42]Chevalier et al. (1999), [43]Bloser et al. (2000), [44]Chevalier et al. (1999), [45]Maccarone & Coppi (2003a), [46]Galloway et al. (2001), [47]Barret et al. (2000), [48]Galloway at al. (2004), [49]Thompson et al. (2005), [50]Mignani et al. (2002), [51]Burderi et al. (2002), [52]Pavlinsky et al. (2001), [53]Cackett et al. (2006), [54]Molkov et al. (2005), [55]Wijnands & van der Klis (1999a), [56]Jonker et al. (2004), [57]Wijnands & van der Klis (1999b), [58]Revnivtsev, Borozdin & Emelyanov (1999), [59]Tomsick et al. (2004), [60]Galloway et al. (2005), [61]Poutanen (2006), [62]Jonker et al. (2005a), [63]Campana et al. (2005), [64]Campana et al. (2003), [65]Gierliński & Poutanen (2005), [66]Wijnands (2003), [67]Krauss et al. (2005), [68]Strohmayer et al. (2003).

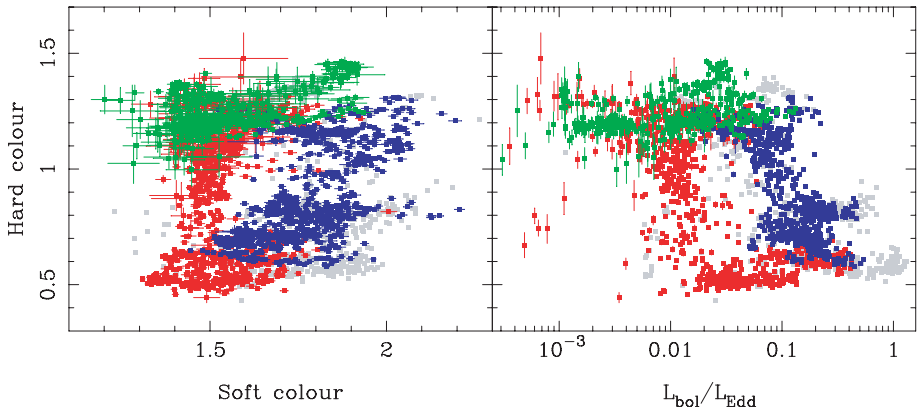

Figure 1. Combined colour–colour and colour–luminosity plots for the *RXTE* PCA data of all atoll sources with $N_H < 3 \times 10^{22}$ cm^{-2}. It is clear that two distinct tracks have emerged, the red track occurring in the figure shows a vertical transitions highlighting that only the higher energies appear to be softening, whilst a diagonal track is highlighted in blue, suggesting the spectrum is softening at all energies, with the millisecond pulsars in green overlaid on a grey back drop of all data. It should be noted that an individual source will only follow one of these tracks.

at which the hard–soft transition occurs varies considerably in the same object (e.g. Nowak 1995; Maccarone & Coppi 2003a). Here, the transition luminosity is varying between different objects.

We show this difference in transition behaviour by plotting the colour–colour and colour–luminosity diagrams for each individual source which shows a clear state transition. Those making a vertical transition are shown in Fig. 2, while those making a diagonal transition are shown in Fig. 3. Not all objects have data covering a transition. Some, such as all the millisecond pulsars, are only seen in the hard (island) state (see Fig. 4), others, e.g. 4U 1758−20, are seen only in the soft (banana) branch. Of the ones which do make transitions, showing both hard and soft spectra, the effects of data windowing mean that not all have observations covering the transition period. None the less, the size of the *RXTE* data base mean there are 12 sources which do have enough data to constrain the shape of the transition on the colour–colour diagrams. The remaining sources, where there is insufficient transition data available at present, are included in the background points plotted on each image, but not plotted individually here (they can be seen in Gladstone 2006).

3.1 Hysteresis

The majority of sources have well-defined transition luminosities (to within a factor of 2–3), irrespective of whether the transition is from hard to soft, i.e. on the rising part of the light curve, or from soft to hard, i.e. with a decreasing flux. However, there are two sources where the transitions have a much large scatter in their properties, namely 4U 1608−52 and 4U 1908+005 (Aql X-1). The colour–colour and colour–luminosity diagrams for these are plotted as the bottom two panels in Fig. 2, but it is not clear from the data that these sources should be classed as verticals, so here we examine them in more detail.

These two systems are also the only two (apart from the millisecond pulsars) which show large-scale outbursts. In order to investigate their scatter in transition behaviour, we select simple outbursts from the light curve, where there is a clear fast rise followed by a monotonic decay. From these data, we build a new, simplified colour–luminosity diagram (Fig. 5). The black triangular points show the island state seen on the rise, which looks very similar to the millisecond pulsars (MSPs) (Fig. 4). We then exclude all of the transition

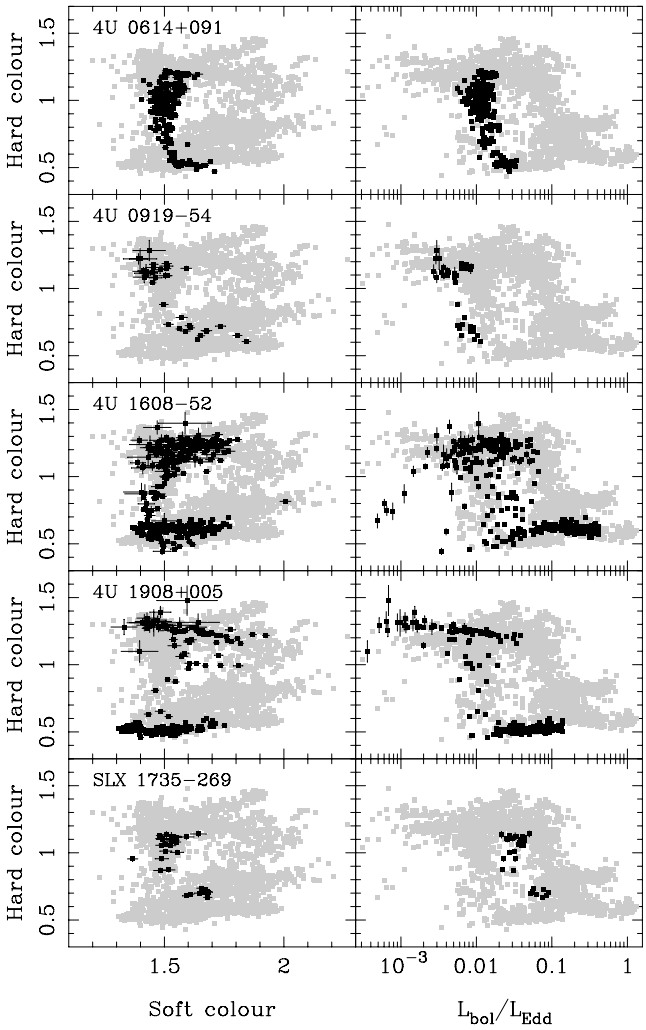

Figure 2. Combined colour–colour and colour–luminosity plots for the *RXTE* PCA data of all atoll sources with $N_H < 3 \times 10^{22}$ cm^{-2} which display a vertical transition from hard to soft state in the colour–colour diagram, plotted against a backdrop of all data.

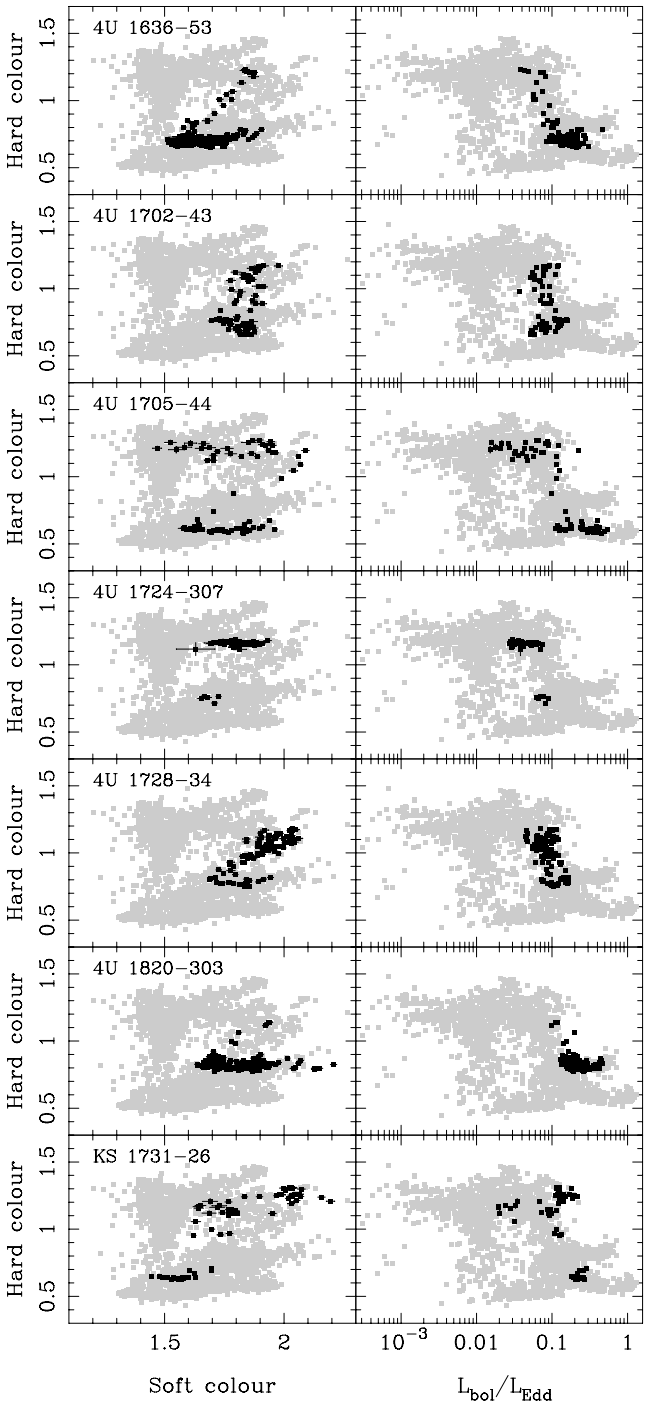

Figure 3. Combined colour–colour and colour–luminosity plots for the *RXTE* PCA data of all atoll sources with $N_H < 3 \times 10^{22}$ cm^{-2} which display a diagonal transition from hard to soft state in the colour–colour diagram, plotted against a backdrop of all data.

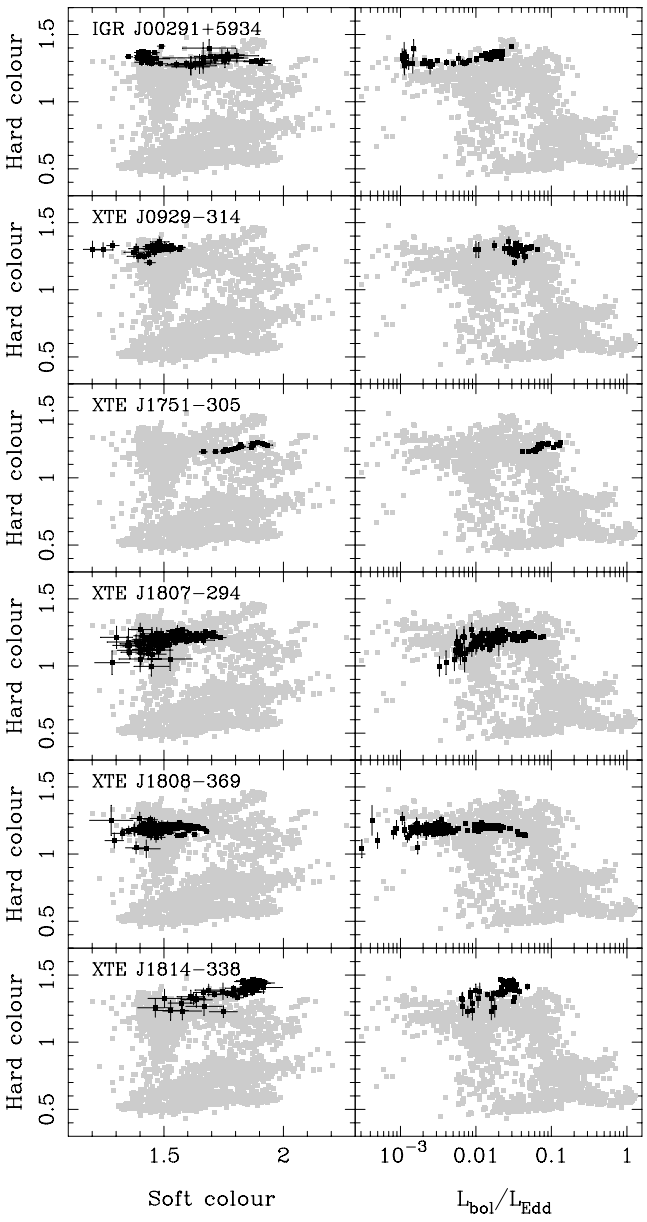

Figure 4. Combined colour–colour and colour–luminosity plots for the *RXTE* PCA data of millisecond pulsars, plotted against a backdrop of all data.

data on the rise/peak of each outburst, and plot the remaining banana branch and transition back to island state on the decay as the blue square points. Plainly, the transition luminosity is much larger in the rise to outburst than during the decay. This effect of hysteresis is also seen in most GBH (e.g. Maccarone & Coppi 2003a). Equally plainly, the decay shows a clear vertical track, confirming the identification of these as verticals. Hence, we speculate that the MSPs are similar objects, and that if the MSP outburst ever reached high enough luminosities to make a transition then this transition would display hysteresis and the colour–colour track during the outburst decay would be vertical.

None of the diagonals show marked hysteresis, though 4U 1705−44 and KS 1731−26 may show a small effect in that their top branch (island state) extends to higher luminosities than seen during the transition (Fig. 3). A similar small hysteresis effect may also be present in the vertical 4U 0919−54.

4 DISCUSSION

There are subtle differences in the spectral evolution of the atolls on the colour–colour and colour–luminosity diagrams: there is the distinction between the transition track (verticals and diagonals), and then within the diagonals there is a difference in spectral hardness of

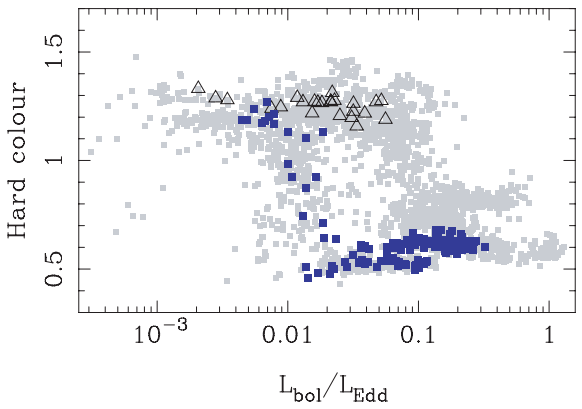

Figure 5. Colour luminosity diagram highlighting the differences in the behaviour of outburst rise and decay (hysteresis) in the bright transients 4U 1608−522 and 4U 1908+005. The colour evolution during the fast rise at the onset of the outburst (black triangles) matches that of the millisecond pulsars, while the outburst decay (blue squares) matches the behaviour of the verticals.

the banana branch, and within the verticals there are objects which show large-scale hysteresis. Here, we examine possible explanations for these effects.

4.1 Inclination

A range of inclinations is expected for these sources, and this could be important for the observed spectrum if the intrinsic emission is not isotropic. Some degree of anisotropy is certainly expected from the accretion disc due to its planar geometry, and as long as the boundary layer has a different angular dependence then the overall spectrum will change as a function of inclination.

To estimate the effects of inclination, we use the spectral model consisting of the disc emission (DISKBB) and the optically thick boundary layer emission, which we model by thermal Comptonization (COMPTT). DG03 showed that the banana branch could be roughly characterized by a disc varying in temperature in the range 1.0–1.5 keV together with an equal luminosity boundary layer with $kT_e = 3$ keV and $\tau = 5$ (see also Revnivtsev & Gilfanov 2006). We use these parameters to model the shape of the banana branch.

We first assume that the boundary layer is isotropic, while the disc normalization varies as $\cos i$ but with angle averaged luminosity equal to that of the boundary layer. Thus, the apparent ratio of disc to boundary layer flux will change as the inclination angle varies. In Fig. 6(a), we show how the banana branch moves on the colour–colour diagram for inclinations of 30°, 60° and 70°. The change is mainly only in the soft colour, with a greater proportion of disc emission shifting the start of the banana branch to lower soft colours. Plainly, this cannot account for either of the two subtle spectral effects seen, but seems to have more potential to explain the different positions of the banana branch amongst the diagonals than the difference between verticals and diagonals.

Examination of some of the individual banana branch spectra of the diagonals showed that the Comptonization temperature of the boundary layer is also changing, and in a way which is correlated with $L_{\rm disc}/L_{\rm BL}$. This could indicate that the boundary layer emission is itself anisotropic, perhaps with a temperature gradient so that it is hotter close to the equatorial plane where the disc hits the neutron star. Fig. 6(b) shows the effect of changing the temperature of the boundary layer from 2.5, 3.0 and 3.5 keV, for inclination angles of 30°, 60° and 70°, respectively. This matches very well with the range of banana branches seen in the diagonals.

Testing this would require knowledge of the inclination, but very few sources have good enough orbital determinations to constrain this. However, any source exhibiting dips must be at fairly high inclination ($i > 70°$), and hence would be expected to have a banana branch starting at fairly large hard and soft colours. This can be seen in the case of 4U 1724−307 (see Fig. 3), a dipping source whose banana branch ranges from 1.65 to 1.75 in soft colour and 0.7 to 0.8 in hard colour. There are three other dipping sources, 4U 1704−30, 4U 1746−37 and 4U 1915−05 (not included in this work), that also support this idea, with each exhibiting large values of both hard and soft colours in the banana state (for details see Gladstone 2006).

4.2 Spin

Burst oscillations and kHz QPOs have finally given observational constraints on LMXB neutron star spins (e.g. the review by van der Klis 2000). For our sample, the inferred range is from 330 to 619 Hz. However, this is unlikely to be the origin of the difference in transition track as the spins seem fairly evenly distributed between the two classes. However, spin could also give a difference in the overall luminosity/temperature of the boundary layer. Lower spin gives a higher relative speed between the inner edge of the disc and the surface, leading to a lower $L_{\rm disc}/L_{\rm BL}$ ratio and a higher boundary layer temperature, as required for the different banana branch hard colours seen. Thus, it seems likely that some combination of spin and inclination effects is responsible for the different banana branches seen in the diagonals, but neither is likely to explain the origin of the two different types of transition behaviour.

4.3 Transient behaviour and hysteresis

Of the subsample of systems with data covering the transition, the publicly available All Sky Monitor (ASM) and/or PCA Galactic Bulge long-term light curves show large-scale transient outbursts only in 4U 1608−52, 4U 1908+005 and all the millisecond pulsars (see Table 1). This is very intriguing as 4U 1608−52 and 4U 1908+005 are both verticals. However, examination of the long-term light curves of the other verticals clearly shows that these objects do not undergo dramatic outbursts, so this cannot be the origin of the vertical/diagonal distinction.

However, 4U 1608−52 and 4U 1908+005 are also the only objects to show clear large-scale hysteresis. Thus, it seems possible that the hysteresis is linked to large amplitude outbursts. There are no counterexamples i.e. no systems that show major disc outbursts (which push the accretion rate high enough to make a spectral transition) which do not show hysteresis. All the millisecond pulsar outbursts remain in the hard state, and all other atoll sources with enough data to delineate the transition and hence constrain hysteresis do not exhibit major outbursts.

This hypothesis can be tested on the black hole LMXB systems. Unlike the atolls, none of these sources is persistent (McClintock & Remillard 2006). This distinction in disc instability behaviour between black holes and neutron stars can be broadly explained in the context of the hydrogen ionization models. Neutron stars are lower in mass than black holes, so for the same companion star to overflow its Roche lobe requires a smaller binary orbit for a neutron star compared to a black hole. Smaller orbital separation means a smaller disc due to tidal truncation. The size of the disc, together with the mass-loss rate from the companion star (determined by its evolutionary state), determines the temperature of the coolest part of

the disc. Thus, the smaller neutron star systems are less likely to have a disc which can drop below the hydrogen ionization temperature required to trigger the disc instability (King, Kolb & Szuszkiewicz 1997; King & Ritter 1998; Dubus et al. 1999).

It is well known that most black hole systems show large-scale hysteresis (e.g. Maccarone & Coppi 2003a). Thus, they support the idea above that hysteresis is linked to large amplitude outbursts. Even more support comes from the one obvious exception, which is Cyg X−1. This does not show hysteresis during its hard/soft transitions, and is of course a persistent (HMXRB) source (e.g. Maccarone & Coppi 2003a; DG03).

Maccarone & Coppi (2003a) also suggested that hysteresis could be linked to large-scale outbursts, but with only Cyg X−1 as a counterexample, the connection to outbursts is not quite so unambiguous. Cyg X−1 is also one of the few known GBH with a high-mass companion, so there is the possibility that its accretion structure is somewhat different due to lower angular momentum material from a stellar wind. By contrast, with the neutron stars being generally stable to the hydrogen ionization trigger for the disc outbursts, there are many counterexamples, all with low-mass companions. We can also rule out the alternative origin for hysteresis discussed by Maccarone & Coppi (2003a), namely that it is produced simply by a difference in behaviour in low-mass X-ray binaries between a hard-to-soft transition on the rising part of the light curve, and a soft-to-hard transition as the flux decreases. Most of the sources shown in Figs 3 and 2 make the transition in both directions, and do not show large-scale hysteresis (though there are smaller scale effects, consistent with the difference in environment: Meyer-Hofmeister, Liu & Meyer 2005). Instead, hysteresis is seen where the mass accretion rate changes dramatically (from $\sim L/L_{\rm Edd} \ll 10^{-4}$ to $\gtrsim 0.1$). We speculate that the accretion flow is able to access non-equilibrium states during the rapid changes in accretion disc structure caused by the disc instability.

Thus, the neutron stars clearly show a one-to-one correlation between the dramatic large amplitude outbursts triggered by the disc instability and hysteresis, consistent with this being the origin of hysteresis. This predicts that the millisecond pulsar outbursts should also show hysteresis if their accretion rate at the outburst peak ever goes high enough to trigger a spectral transition (in which case we would expect them to also be verticals, along with 4U 1608−52 and 4U 1908+005). However, there is no such one-to-one correlation between outbursts and transition behaviour (vertical/diagonal), so we explore further aspects of the systems below.

4.4 Binary system parameters

Table 1 shows the binary parameters where these are known. We first explore whether there is any correlation between transition behaviour and binary period (which is a tracer of companion type, and also of superburst behaviour: Cumming 2003). For the verticals, the periods span a large range, from 1 h for the persistent sources 4U 0614+091 and 4U 0919−54 through to 19 and 288 h for the transients 4U 1608−52 and 4U 1908+005. This distinction is as expected from the disc instability model (wide binary implies a much larger disc, so a cooler outer edge which is more likely to trigger the hydrogen instability). If the millisecond pulsars are also verticals then these fill in the period distribution from 40 min to 4 h. There is very little data to compare this to the diagonals, as only two have periods (11 min and 3.9 h), but the broad span seen from the verticals encompasses most of the binary periods seen in atolls, so binary period alone is unlikely to be the origin of the transition track dichotomy.

4.5 Long-term mass accretion rate

The distinction between millisecond pulsars, which plainly retain a residual magnetic field channelling the flow, and other atolls which do not show pulsations is most probably due to the long timescale mass accretion rate (Cumming, Zweibel & Bildsten 2001). Plausibly, high accretion rates can bury the magnetic field below the neutron star surface, but the very low average mass accretion rate in the millisecond pulsars is insufficient to bury the field (Cumming et al. 2001). Thus, there is a potential physical mechanism for the long-term mass accretion rate to change the properties of the accretion flow.

We estimate the long-term mass accretion rate, $\langle \dot{m} \rangle$ (or corresponding average luminosity, $\langle L_{\rm bol}/L_{\rm Edd} \rangle$), for all of the systems from the observed X-ray emission. The PCA data give estimates for $L_{\rm bol}$ through spectral fitting, but the light curves are highly incomplete, so the data cannot simply be used as an indicator of the long-term average mass accretion rate. By contrast, the *RXTE* ASM gives an almost continuous light curve for every bright X-ray source

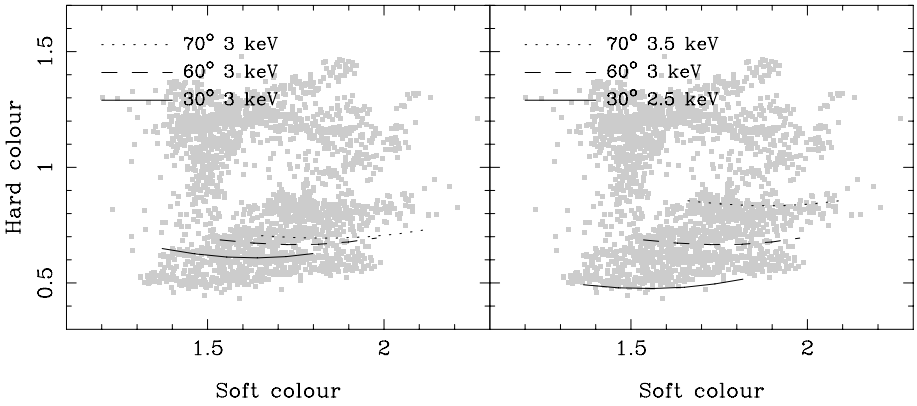

Figure 6. Colour–colour diagrams showing the effect of inclination on the position of the banana branch. The inclination is 30° (solid curves), 60° (dashed curves) and 70° (dotted curves). Each curve represents the disc plus boundary layer model, for the range of disc temperatures of 1.0–1.5 keV (see text for details). In Panel (a), the disc emission is assumed to be angle dependent, while the boundary layer emission is isotropic, with constant temperature of 3 keV. In Panel (b), the boundary layer emission is assumed to be anisotropic, with higher observed temperature closer to the equator. The three curves correspond to the same inclination angles as in Panel (a), but this time the boundary layer temperature is 2.5, 3.0 and 3.5 keV for increasing angles, respectively.

in its field of view, but its lack of spectral resolution means that going from count rate to $L_{\rm bol}$ is highly uncertain. Hence, we combine the two approaches. We use the PCA light curve to define the average $\langle L_{\rm bol}/L_{\rm Edd}\rangle$ during these observations, then select the simultaneous ASM points to find the average ASM count rate during the PCA observations. The ratio of this to the full ASM light curve gives the correction for the incompleteness of the PCA observations.

This approach works well unless the source becomes very faint, in which case contamination of the ASM by other nearby sources and/or Galactic ridge emission can be a problem. The only sources for which this is an issue are the transients i.e. the verticals 4U 1608−52 and 4U 1908+005 and all the millisecond pulsars. The outbursts of 4U 1608−52 and 4U 1908+005 are so bright that they dominate the average of the ASM light curves. However, this is not the case for the millisecond pulsars, so for these we use a different approach. Here, we use the PCA data alone, which have good outburst coverage, assuming that the source intensity is negligible in the periods outside the known outbursts. The results of both the millisecond pulsars and atoll sources are shown in Table 2.

It can be seen that there is a systematic difference between the three classes of sources. The millisecond pulsars have the lowest $\langle L_{\rm bol}/L_{\rm Edd}\rangle$, then the verticals, then the diagonals. Thus, it seems possible that this is the origin of the difference in transition properties. The millisecond pulsars' low $\langle \dot{m}\rangle$ allows the field to diffuse out of the crust, and to be strong enough to collimate the flow and produce pulsations. One possibility might be that while the high $\langle \dot{m}\rangle$ of the diagonals suppresses the field entirely, the medium $\langle \dot{m}\rangle$ in the verticals allows some field to diffuse out. But, the verticals show no trace of pulsation, so the magnetic field cannot collimate any significant part of the flow.

One way around these pulsation limits is to separate the field and accretion flow. Any non-spherical accretion flow will predominantly bury the field in the region of the flow, leaving the field to escape in regions with little accretion. Even the hot accretion flow envisaged for the hard island states favours the equatorial plane, with a geometry which is more like a thick disc than a truly spherical flow (e.g. Narayan & Yi 1995). This nicely circumvents the pulsation limits, but then there is no interaction between the magnetic field and the flow, and so no physical mechanism to change the behaviour of the transition.

However, one aspect of the system that a polar magnetic field could affect is the jet. The most recent numerical simulations of the accretion flow magnetohydrodynamics show a causal link between the jet and accretion flow (Hawley & Krolik 2006; McKinney 2006), so this might give an indirect link between the magnetic field and accretion flow properties. One way to test this is to look at the radio emission from these systems. While theoretical models of jets are not well developed, we can use the observed GBH behaviour as a template. These show a clear correlation between radio and X-ray luminosity in their low/hard state, showing that $L_{\rm X}/L_{\rm Edd}$ is important in determining the power of the jet (Gallo et al. 2006). Hence, to see whether there are differences in the jet emission between the millisecond pulsars, verticals and diagonals we need to compare the radio emission at the same $L_{\rm X}/L_{\rm Edd}$. Hysteresis gives potential problems, so ideally the comparison would be between persistent verticals and diagonals in the hard island state at the same $L_{\rm X}$. However, there is very little data to make this comparison, with only 4U 0614+091 and 4U 1728−34 for the persistent verticals and diagonals, respectively, and these do not overlap in $L_{\rm X}$ (Migliari & Fender 2006). Thus, we speculate that the origin of the difference in transition behaviour between the verticals and diagonals is due to the presence of some magnetic field at the pole in the verticals which affects the accretion flow indirectly through jet formation, by contrast to the diagonals which have higher mass accretion rates, sufficient to bury the field everywhere.

Table 2. Long-term average luminosity revealing a distinct break between MSP and atoll sources as well as a more subtle break between sources where the hard–soft transition is approximately vertical on a colour–colour diagram (V) and those where it makes a diagonal track (D).

Source name	Source type	$\langle L_{\rm bol}/L_{\rm Edd}\rangle$
IGR J00291+5934	MSP	1.4×10^{-5}
XTE J0929−314	MSP	1.4×10^{-4}
XTE J1751−305	MSP	5.2×10^{-5}
XTE J1807−294	MSP	2.7×10^{-4}
XTE J1808−369	MSP	6.7×10^{-5}
XTE J1814−338	MSP	1.6×10^{-4}
4U 0614+091	V	3.2×10^{-3}
4U 0919−54	V	3.1×10^{-3}
4U 1608−52	V	6.6×10^{-3}
4U 1908+005	V	3.7×10^{-3}
SLX 1735−269	V	1.6×10^{-3}
4U 1636−53	D	4.4×10^{-2}
4U 1702−43	D	7.8×10^{-3}
4U 1705−44	D	1.9×10^{-2}
4U 1724−307	D	7.3×10^{-3}
4U 1728−34	D	1.9×10^{-2}
4U 1820−303	D	1.3×10^{-1}
KS 1731−26	D	3.4×10^{-2}

5 CONCLUSIONS

The atolls and millisecond pulsars are consistent with showing the same overall spectral evolution with changing mass accretion rate, but there are some subtle differences. The spectral shape of the soft (banana) branch shows subtle variations from object to object, most probably due to combination of inclination and spin changing the ratio of the observed disc to boundary layer luminosity, and boundary layer temperature. However, there are also clear differences in behaviour during the hard/soft transition which point to a more fundamental distinction. The data show two types of sources, those where the transition makes a vertical track on the colour–colour diagram, and occurs at $L/L_{\rm Edd} \sim 0.02$, and those which make a diagonal track on the colour–colour diagram with the transition at $L/L_{\rm Edd} \sim 0.1$. There are hysteresis effects in individual sources which introduce dispersion in the transition luminosity, but these are large *only* for the outbursting atolls (which are both verticals). Splitting these outbursts into the rapid rise and slow decay phases shows that the rapid rise looks like the millisecond pulsars (so they are probably also verticals) while the slow decay looks like the persistent verticals. Thus, it seems likely that large-scale hysteresis effects are only seen in sources where the disc structure changes rapidly due to the onset of the hydrogen ionization instability. This is also consistent with the observed black hole behaviour. The association of the millisecond pulsars with verticals suggests that the difference in transition is ultimately linked to the surface magnetic field and, indeed, all the verticals have long-term mass accretion rates which are smaller than those of the diagonals, though not as small as those of the millisecond pulsars. Thus, the verticals could have some small B field which is able to affect the inner accretion flow, but this must be indirect as otherwise these systems would also show pulsations. We speculate that the physical link between the magnetic field (predominantly

polar) and accretion flow (predominantly equatorial) may be due to the changes in the jet, which would be testable with more radio data on these sources.

ACKNOWLEDGMENTS

This research has made use of data obtained through the High Energy Astrophysics Science Archive Research Centre Online Service, provided by the NASA/Goddard Space Flight Center.

REFERENCES

Angelini L., White N. E., Nagase F., Kallman T. R., Yoshida A., Takeshima T., Becker C., Paerels F., 1995, ApJ, 449, L41
Bałucińska-Church M., Church M. J., Smale A. P., 2004, MNRAS, 347, 334
Barret D., Vedrenne G., 1994, ApJS, 92, 505
Barret D., Olive J. F., Boirin L., Done C., Skinner G. K., Grindlay J. E., 2000, ApJ, 533, 329
Barret D., Olive J. F., Oosterbroek T., 2003, A&A, 400, 643
Bloser P. F., Grindlay J. E., Barret D., Boirin L., 2000, ApJ, 542, 989
Burderi L. et al., 2002, ApJ, 574, 930
Cackett E. M. et al., 2006, MNRAS, 369, 407
Campana S., Ravasio M., Israel G. L., Mangano V., Belloni T., 2003, ApJ, 594, L39
Campana S., Ferrari N., Stella L., Israel G. L., 2005, A&A, 434, L9
Chevalier C., Ilovaisky S. A., Leisy P., Patat F., 1999, A&A, 347, L51
Christian D. J., Swank J. H., 1997, ApJS, 109, 177
Cornelisse R., Heise J., Kuulkers E., Verbunt F., in't Zand J. J. M., 2000, A&A, 357, L21
Courvoisier T. J.-L., Parmar A. N., Peacock A., Pakull M., 1986, ApJ, 309, 265
Cumming A., 2003, ApJ, 595, 1077
Cumming A., Zweibel E., Bildsten L., 2001, ApJ, 557, 958
Di Salvo T., Iaria R., Burderi L., Robba N. R., 2000, ApJ, 542, 1034
Di Salvo T., Iaria R., Méndez M., Burderi L., Lavagetto G., Robba N. R., Stella L., van der Klis M., 2005, ApJ, 623, L121
Díaz Trigo M., Parmar A. N., Boirin L., Méndez M., Kaastra J. S., 2006, A&A, 445, 179
Done C., Gierliński M., 2003, MNRAS, 342, 1041 (DG03)
Done C., Gierliński M., 2006, MNRAS, 367, 659
Dubus G., Lasota J.-P., Hameury J.-M., Charles P., 1999, MNRAS, 303, 139
Emelyanov A. N., Revnivtsev M. G., Aref'ev V. A., Sunyaev R. A., 2002, Astron. Lett., 28, 12
Falanga M., Farinelli R., Goldoni P., Frontera F., Goldwurm A., Stella L., 2004, A&A, 426, 979
Falcke H., Körding E., Markoff S., 2004, A&A, 414, 895
Farinelli R. et al., 2003, A&A, 402, 1021
Fender R. P., Hendry M. A., 2000, MNRAS, 317, 1
Gallo E., Fender R. P., Miller-Jones J. C. A., Merloni A., Jonker P. G., Heinz S., Maccarone T. J., van der Klis M., 2006, MNRAS, 370, 1351
Galloway D. K., Chakrabarty D., Muno M. P., Savov P., 2001, ApJ, 549, L85
Galloway D. K., Cumming A., Kuulkers E., Bildsten L., Chakrabarty D., Rothschild R. E., 2004, ApJ, 601, 466
Galloway D. K., Markwardt C. B., Morgan E. H., Chakrabarty D., Strohmayer T. E., 2005, ApJ, 622, L45
Garcia M. R., McClintock J. E., Narayan R., Callanan P., Barret D., Murray S. S., 2001, ApJ, 553, L47
Gierliński M., Done C., 2002, MNRAS, 331, L47
Gierliński M., Poutanen J., 2005, MNRAS, 359, 1261
Gladstone J. C., 2006, MSc thesis, University of Durham (web version available at http://astro.dur.ac.uk/∼jgetty/MSc_thesis.pdf)
Hasinger G., van der Klis M., 1989, A&A, 225, 79
Hawley J. F., Krolik J. H., 2006, ApJ, 641, 103
Homer L., Charles P. A., Naylor T., van Paradijs J., Auriere M., Koch-Miramond L., 1996, MNRAS, 282, L37
in't Zand J. J. M., Strohmayer T. E., Markwardt C. B., Swank J., 2003a, A&A, 409, 659
Jonker P. G., van der Klis M., Homan J., Wijnands R., van Paradijs J., Méndez M., Kuulkers E., Ford E. C., 2000, ApJ, 531, 453
Jonker P. G. et al., 2001, ApJ, 553, 335
Jonker P. G., van der Klis M., Kouveliotou C., Méndez M., Lewin W. H. G., Belloni T., 2003, MNRAS, 346, 684
Jonker P. G., Galloway D. K., McClintock J. E., Buxton M., Garcia M., Murray S., 2004, MNRAS, 354, 666
Jonker P. G., Steeghs D., Nelemans G., van der Klis M., 2005a, MNRAS, 356, 621
Jonker P. G., Campana S., Steeghs D., Torres M. A. P., Galloway D. K., Markwardt C. B., Chakrabarty D., Swank J., 2005b, MNRAS, 361, 511
Juett A. M., Chakrabarty D., 2003, ApJ, 599, 498
Kallman T. R., Angelini L., Boroson B., Cottam J., 2003, ApJ, 583, 861
King A. R., Ritter H., 1998, MNRAS, 293, L42
King A. R., Kolb U., Szuszkiewicz E., 1997, ApJ, 488, 89
Krauss M. I. et al., 2005, ApJ, 627, 910
Krolik J. H., Hawley J. F., Hirose S., 2005, ApJ, 622, 1008
Liu Q. Z., van Paradijs J., van den Heuvel E. P. J., 2001, A&A, 368, 1021
McClintock J. E., Remillard R. A., 2006, csxs.book, 157
McClintock J. E., Narayan R., Rybicki G. B., 2004, ApJ, 615, 402
McKinney J. C., 2006, MNRAS, 368, 1561
Maccarone T. J., Coppi P. S., 2003a, MNRAS, 338, 189
Maccarone T. J., Coppi P. S., 2003b, A&A, 399, 1151
Manchanda R. K., Rao A. R., 2001, Adv. Space Res., 28, 337
Meyer-Hofmeister E., Liu B. F., Meyer F., 2005, A&A, 432, 181
Migliari S., Fender R. P., 2006, MNRAS, 366, 79
Migliari S. et al., 2003a, MNRAS, 342, 909
Migliari S., van der Klis M., Fender R. P., 2003b, MNRAS, 345, L35
Mignani R. P., Chaty S., Mirabel I. F., Mereghetti S., 2002, A&A, 389, L11
Miller J. M. et al., 2002, BAAS, 34, 1206
Miller J. M. et al., 2006, ApJ, 646, 394
Miniutti G., Fabian A. C., Miller J. M., 2004, MNRAS, 351, 466
Mitsuda K. et al., 1984, PASJ, 36, 741
Molkov S. V., Grebenev S. A., Lutovinov A. A., 2000, A&A, 357, L41
Molkov S., Revnivtsev M., Lutovinov A., Sunyaev R., 2005, A&A, 434, 1069
Muno M. P., Remillard R. A., Chakrabarty D., 2002, ApJ, 568, L35
Narayan R., Heyl J. S., 2002, ApJ, 574, L139
Narayan R., Yi I., 1995, ApJ, 452, 710
Nelemans G., Jonker P. G., Marsh T. R., van der Klis M., 2004, MNRAS, 348, L7
Nishiuchi M. et al., 2000, Adv. Space Res., 25, 391
Nowak M. A., 1995, PASP, 107, 1207
Oosterbroek T., Parmar A. N., Sidoli L., in't Zand J. J. M., Heise J., 2001, A&A, 376, 532
Owens A., Oosterbroek T., Parmar A. N., 1997, A&A, 324, L9
Park S. Q., Miller J. M., McClintock J. E., Murray S. S., 2005, ApJ, 618, L45
Parkinson P. M. S. et al., 2003, ApJ, 595, 333
Parmar A. N., Oosterbroek T., Del Sordo S., Segreto A., Santangelo A., Dal Fiume D., Orlandini M., 2000, A&A, 356, 175
Parmar A. N., Oosterbroek T., Boirin L., Lumb D., 2002, A&A, 386, 910
Pavlinsky M. N., Grebenev S. A., Lutovinov A. A., Sunyaev R. A., Finoguenov A. V., 2001, Astron. Lett., 27, 297
Piro A. L., Bildsten L., 2005, ApJ, 629, 438
Poutanen J., 2006, Adv. Space Research, 38, 2697
Revnivtsev M. G., Gilfanov M. R., 2006, A&A, 453, 253
Revnivtsev M., Borozdin K., Emelyanov A., 1999, A&A, 344, L25
Schultz N. S., 1999, ApJ, 511, 304
Shaposhnikov N., Titarchuk L., 2004, ApJ, 606, L57
Shaposhnikov N., Titarchuk L., Haberl F., 2003, ApJ, 593, L35
Sidoli L., La Palombara N., Oosterbroek T., Parmar A. N., 2005, A&A, 443, 223
Smale A. P., Church M. J., Bałucińska-Church M., 2002, ApJ, 581, 1286
Strohmayer T. E., Markwardt C. B., Swank J. H., in't Zand J., 2003, ApJ, 596, L67

Sunyaev R., Revnivtsev M., 2000, A&A, 358, 617
Thompson T. W. J., Rothschild R. E., Tomsick J. A., Marshall H. L., 2005, ApJ, 634, 1261
Tomsick J. A., Gelino D. M., Halpern J. P., Kaaret P., 2004, ApJ, 610, 933
van der Klis M., 2000, ARA&A, 38, 717
Wang Z., Chakrabarty D., 2004, ApJ, 616, L139
Wardziński G., Zdziarski A. A., Gierliński M., Eric Grove J., Jahoda K., Neil Johnson W., 2002, MNRAS, 337, 829
Wijnands R., 2001, ApJ, 554, L59
Wijnands R., 2003, ApJ, 588, 425
Wijnands R., van der Klis M., 1999a, A&A, 345, L35
Wijnands R., van der Klis M., 1999b, ApJ, 522, 965
Wijnands R., Strohmayer T., Franco L. M., 2001, ApJ, 549, L71
Wilson C. A., Patel S., Kouveliotou C., Jonker P. G., van der Klis M., Lewin W. H. G., Belloni T., Méndez M., 2003, ApJ, 596, 1220
Wolff M. T., Hertz P., Wood K. S., Ray P. S., Bandyopadhyay R. M., 2002, ApJ, 575, 384
Wolff M. T., Becker P. A., Ray P. S., Wood K. S., 2005, ApJ, 632, 1099
Yao Y., Wang Q. D., 2005, ApJ, 624, 751
Zdziarski A. A., Johnson W. N., Magdziarz P., 1996, MNRAS, 283, 193

This paper has been typeset from a TEX/LATEX file prepared by the author.